Preprints (www.preprints.org) | NOT PEER-REVIEWED | Posted: 24 December 2018 doi:10.20944/preprints201812.0290.v1

Peer-reviewed version available at *Materials* **2019**, *12*, 382; doi:10.3390/ma12030382

Article

Bottom-up self-assembled supramolecular structures built by STM at solid/liquid interface

Quirina Ferreira [1]*, Catarina L. Delfino [1], Jorge Morgado [1,2] and Luís Alcácer [1]

[1] Instituto de Telecomunicações, Instituto Superior Técnico, Av. Rovisco Pais, 1049-001 Lisboa, Portugal 1;
[2] Bioengineering Department, Instituto Superior Técnico, University of Lisbon, Av.Rovisco Pais,1049-001, Lisbon, Portugal
* Correspondence: quirina.ferreira@lx.it.pt; Tel.: +351-218-418-094

Abstract: The development of organic devices has been focused in their miniaturization in order to obtain denser and faster electronic circuits. The challenge is to build the devices adding atom by atom or molecule by molecule until the desired structure is achieved. To do this job, techniques able to see and manipulate matter at this scale are needed. Scanning tunneling microscopy has been the selected technique by scientists to develop smart and functional unimolecular devices. This review article compiles the lastest developments in this field giving examples of supramolecular systems monitored and fabricated at molecular scale by bottom-up approaches using STM at solid/liquid interface.

Keywords: Scanning tunneling microscopy; unimolecular electronics; molecular device; monolayer; coordination chemistry, interfaces, nanotechnology

1. Introduction

The development of functional and smart organic materials for optoelectronics has been a challenge for researchers in the field of nanoengineering. The interest lies in the possibility of designing and developing materials with a specific functionality and integrating them in an electronic device, such as, sensors [1], light emitting diodes [2], photovoltaic cells [3,4], transistors [5] and many others. Research has been focused on low-cost and versatile methods of material production combined with the necessity of making smaller and denser electronic devices. Molecular electronics is a viable solution to overcome this challenge using individual molecules or molecular assemblies as the active components of an electronic circuit [6,7]. Over the last decade, expectations for this field were driven by i) the possibility of these molecules becoming alternatives to silicon-based technology, that is still-to-this-day the core of the integrated electronic circuits; ii) several synthesis and manufacturing processes that have already been adapted and several techniques made available that allow the preparation of high quality molecular films and the characterization of these devices; iii) the ability to design and model structures at a molecular level; and iv) the application and integration of molecular devices in real-life applications.

A molecular device is an assembly of molecular elements designed to behave in a certain manner, operating in a specific capacity and developed for a precise function. Each element contributes with a single function cooperating for the performance of the complex molecular device. The individual components can operate as a result of an external stimulus and can be easily replaced by other elements in order to accomplish a desired function. Each element can be individually stimulated as a result of an external source. This idea was introduced for the first time by K. E. Drexler[8]. He proposed a nanodevice construction using a stepwise method adding atom by atom until a complex supramolecular structure was achieved, to which he called "assembler". This idea has been implemented and revolutionized the manufacture of electronic devices opening the door to new complex structures that have never been developed because traditional top-down methods do not allow it. With the experiments of the Nobel Prize in Chemistry of C.J. Pederson[9], D.J. Cram[10] and J.-M. Lehn[11] in 1987 about supramolecular chemistry, new molecular devices have been developed

© 2018 by the author(s). Distributed under a Creative Commons CC BY license.

Preprints (www.preprints.org) | NOT PEER-REVIEWED | Posted: 24 December 2018 doi:10.20944/preprints201812.0290.v1

Peer-reviewed version available at Materials 2019, 12, 382; doi:10.3390/ma12030382

by bottom-up approaches, connecting self-assembly molecules to obtain larger structures. Recently, in 2016, the Nobel Prizes in Chemistry, J.-P. Sauvage[12], Sir J.F. Stoddart[13] and B. L. Feringa[14] showed how it is possible to build and manipulate nanomachines. Thereby consolidating the idea that the molecule by molecule approach allows the fabrication of complex electronic devices.

The development of materials at the molecular level requires specific fabrication techniques that allow visualization and manipulation of matter at this scale. This is the point that this review article wants to address, showing how molecular devices can be fabricated using a bottom-up approach based on atom by atom or molecule by molecule assembly until functional and complex structure is achieved. Scanning Tunneling Microscopy (STM) is the elected technique to play with matter at the atomic level. Namely, STM has been used to monitor in real-time the formation of highly organized self-assembled monolayers where the molecules arrange themselves into packed 2D crystals fully covering the surface of the substrate on which they are deposited. Several high resolution STM images of the formation of molecular systems by self-assembly have been reported revealing the parameters involved in the monolayer formation: whether they are physical parameters (e.g. concentration of solutes, wettability, contact angles, superficial tension, temperature variations) or chemical parameters (e.g. molecule structure, orbital configuration). All these monolayer properties are important for the design of organic devices.

Recently, STM has been used to build molecular systems with multicomponents, e.g. self-assembled monolayers with more than one molecular element or vertical supramolecular structures synthesized *in-situ* [6,7,14,15]. The experiments are called STM at solid/liquid interface when they occur at interface with a high boiling point solvent which is added to a conductive and atomically flat substrate. Ideally, this drop should be preserved during long periods of time (several hours) to allow enough time to see and monitor a monolayer in real time. The drop works as a nanolab where the molecules can be added to form one or more monolayers, as it is schematized in Figure 1. This nanolab allows the *in-situ* synthesis of complex supramolecular structures, where each step can be monitored by high resolution images [6,7]. Each system requires specific conditions: nature of substrate, solvent, temperature, concentration and characteristics of tip. The solvent has an important role, since it can participate in the formation of monolayer coadsorbing with the molecules that are being deposited [16**?**].

Preprints (www.preprints.org) | NOT PEER-REVIEWED | Posted: 24 December 2018 doi:10.20944/preprints201812.0290.v1

Peer-reviewed version available at Materials 2019, 12, 382; doi:10.3390/ma12030382

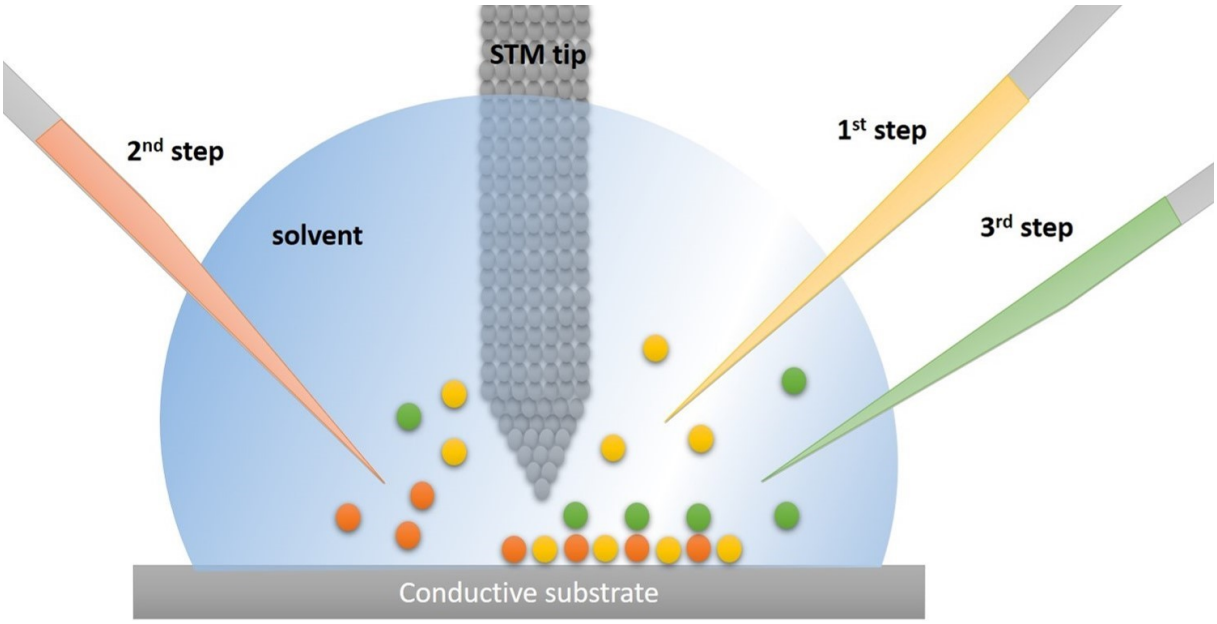

Figure 1. Schematic representation of a stepwise building of supramolecular structures built by STM at solid/liquid interface. Each step corresponds to one molecule or molecular system which can be added individually and monitored by high resolution images. The experiments occur inside a drop of a high boiling point solvent which is added on the top of a conductive substrate and allows the phased addition of molecules.

2. Molecular 2D patterned arrays

Conductive organic self-assembly and self-organized monolayers are the starting point of organic device building. They are spontaneously formed on a substrate, usually on a conductive substrate, and they can be composed of one or more than one type of molecules, depending on the application. Due to the high reproducibility of this technique, it is easy to implement self-assembly materials in the development of large-scale devices. The molecular ordering is strongly dependent on the intra- and intermolecular interactions, temperature, concentration, solvent and also the chemical/physical interactions with substrate ([17] and the references in there). STM is the perfect tool to study all of these factors while monitoring the monolayer formation in real time through high resolution images. The fabrication of several monolayers have been reported using STM to see the molecular organization and in some cases to manipulate their formation. Experiments at solid/liquid interface have contributed to the development of organic devices at room temperature, under atmospheric pressure and in some cases under aqueous environments. This represents an important progress of the development of materials at a sub-molecular scale taking into account that most of devices operate in these conditions.

2.1. Polymorphism

In some cases, the monolayer formation can have intermediate metastable phases which correspond to a molecular packing configuration that has not yet reached the equilibrium[18–22]. In particular, the monolayers formed at solid/liquid interface are influenced by the solvent, which in turn can induce polymorphism in the molecular organization. In some cases, the solvent molecules are co-adsorbed with the molecules that are being deposited. In particular, competition between the molecules being deposited and the solvent occurs while the monolayer forms at the solid/liquid interface. Some of these molecules are adsorbed together with the solvent molecules. Competition with the solvent can be seen from the moment that the molecules are being adsorbed on the top of substrate. Ferreira *et al* used STM to visualize the competition effect between zinc porphyrins and tetradecane for more than 2 hours[16]. Figure 2 shows consecutive STM images acquired after 2 hours of the deposition of the molecules, evidencing the coexistence of three metastable phases α, β and γ which

Preprints (www.preprints.org) | NOT PEER-REVIEWED | Posted: 24 December 2018 doi:10.20944/preprints201812.0290.v1

Peer-reviewed version available at Materials 2019, 12, 382; doi:10.3390/ma12030382

correspond to different molecular packing associated with different conformations of porphyrins. The authors attribute the coexistence of these three phases to a competition between the porphyrins and the solvent.

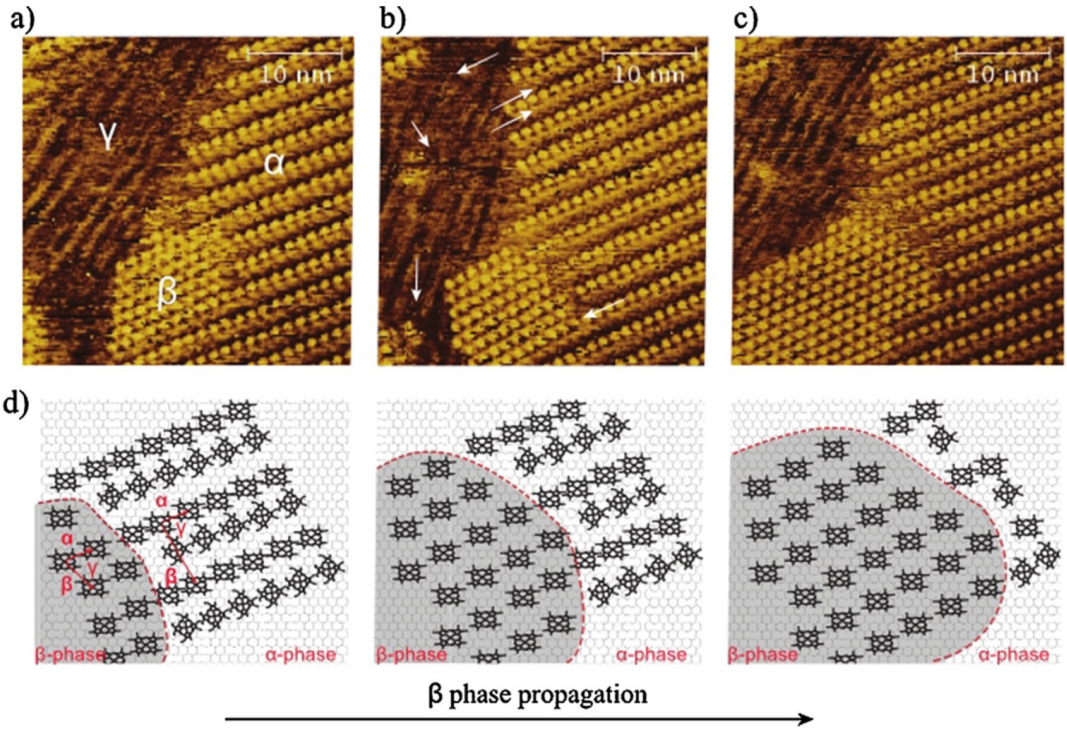

Figure 2. STM images (a), (b) and (c) of ZnOEP adsorption on HOPG were recorded sequentially with 2-minute intervals after 2 hours since the deposition of porphyrin in the tetradecane droplet. These STM images show a polymorphic monolayer with three different co-existing phases, in which the white arrows point to molecules with increased contribution to the signal and a propagation of a β-phase, which is modelled in (d), (e) and (f). (Reprinted with permission from reference [16]. Copyright 2013 Elsevier B.V)

At solid/liquid interface experiments, the equilibrium of a packed monolayer depends on the adsorbed/desorbed molecules and the molecules that remain in the liquid environment [23]. To achieve the stability of the molecular organization, molecules that are being adsorbed compete with the molecules that remains in solution. Consequently, the molecular packing can change from a dense array to a porous packing, as well as from a full packed monolayer to a disorganized array [24,25]. Polimorphism is important in the design of organic devices, since it affects the carrier transport[26]. STM plays an important role in the identification of the metastable phases which can occur during the monolayer formation, since it remains the only technique able to analyze the molecular changes in real time.

2.2. In-situ synthesis

Two-dimensional self-organized monolayers can work as anchor points to obtain vertical structures, bonding molecules one by one. Otsuki *et al.* [15] described the fabrication of labile axial ligands (*i.e.* pyridine) on a template monolayer of zinc porphyrins, deposited beforehand on HOPG. The research group prepared ordered arrays of porphyrins ($H_2(C_{18}OPP)$) and metalloporphyrins ($Zn(C_{18}OPP)$) at HOPG /1-phenyloctane interface. On top of which an Azo (4-(phenylazo)pyridine)) molecule was assembled via axial coordination to the metallic center, both in a *cis*- and *trans*-conformation. From the STM data, porphyrin films were reported as hardly differentiable until the addition of Azo provided a difference in contrast.

Preprints (www.preprints.org) | NOT PEER-REVIEWED | Posted: 24 December 2018 doi:10.20944/preprints201812.0290.v1

Peer-reviewed version available at Materials 2019, 12, 382; doi:10.3390/ma12030382

A few years later, Feringa and co-workers [27] reported on the axial construction of suprastructures with an *in-situ* self-assembly strategy, relying on metalloporphyrins arrays as building units. More specifically, a Zn-tetrakis(meso-dodecyl)porphyrin (ZnTDP) self-assembly monolayer was deposited at the HOPG/n-tetradecane interface and covalently bounded to a meta-substituted pyridine, namely 3-nitropyridine. ZnTDP and the pyridine were also placed together in solution to ensure that axial coordination between the molecules only occured once the porphyrin monolayer was assembled at the interface. Prior to STM imaging the compounds were dissolved in a specific solvent (n-tetradecane) and then a droplet of solution was applied on freshly cleaved HOPG and imaged with STM at room temperature. Upon physisorption of the molecules at the interface, high resolution STM images of well ordered patterned arrays were obtained. Figure 3 *c)* shows the monolayer formed by the porphyrin covalently bonded to the pyridine. After the self-assembly of the monolayer each porphyrin lies flat at the interface by $\Pi - \Pi^*$ stacking over the HOPG substrate. The authors observed a higher ratio of coordinated porphyrins compared with unreacted porphyrins, that was explained by the preference of pyridines with physisorbed porphyrins, rather than with the porphyrins in solution.

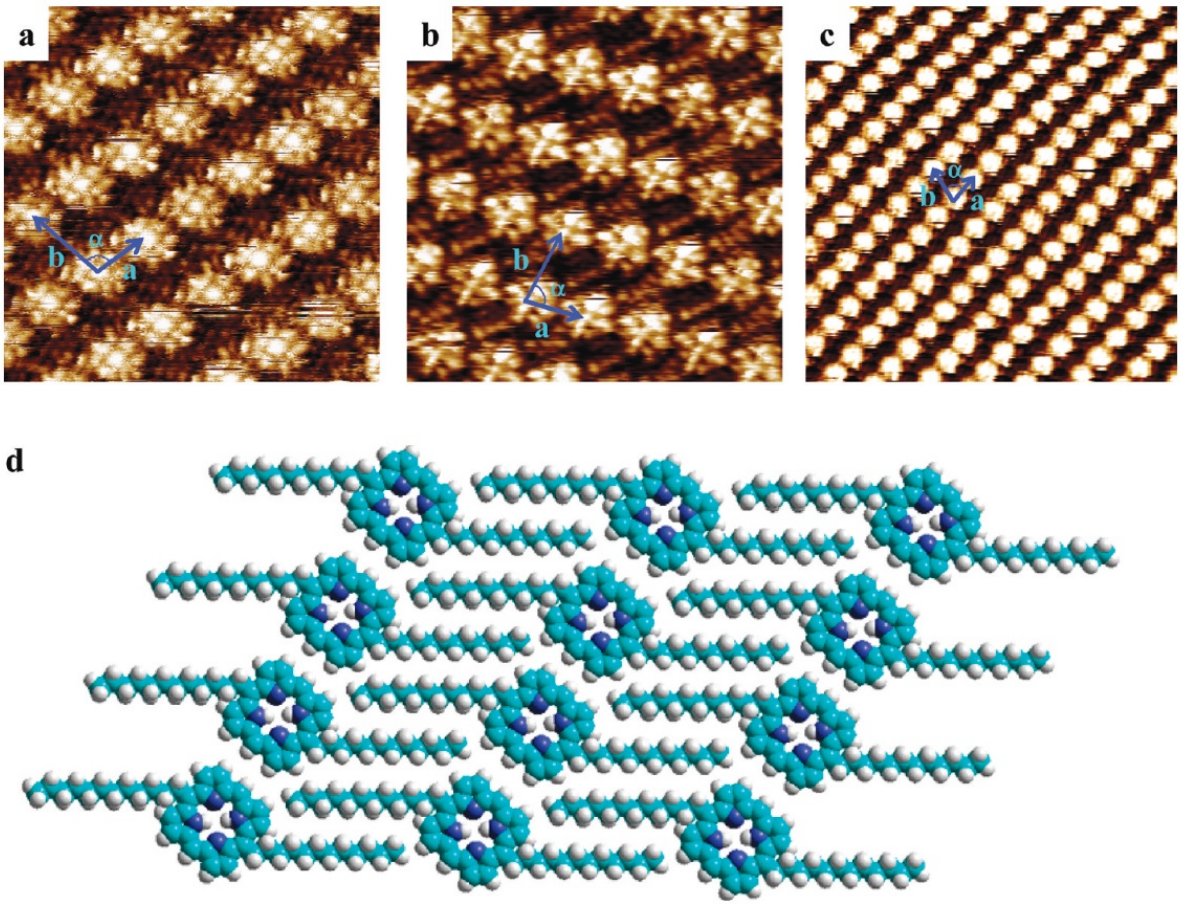

Figure 3. STM images obtained for different self-assembled monolayers: *(a)* monolayer of non-coordinated porphyrin as control, 5,10,15,20-*meso*-tetradodecylporphyrin (TDP) (with 8.1*x*8.1*nm*); *(b)* monolayer of the same porphyrin coordinated with a Zinc metal-ion (ZnTDP) (with 9.3*x*9.3*nm*); *(c)* a monolayer of 3-nitropyridine molecules that were self-assembled and coordinated to the layer underneath, a ZnTDP monolayer (with 20.8*x*20.8*nm*); *(d)* packing arrangement model for TDP assembled on HOPG. (Reprinted with permission from reference [27]. Copyright 2016 American Chemical Society)

This work paved the way to *in-situ* synthesis of supramolecular systems and unimolecular devices [6,7] developed by a layer-by-layer approach.

Preprints (www.preprints.org) | NOT PEER-REVIEWED | Posted: 24 December 2018 doi:10.20944/preprints201812.0290.v1

Peer-reviewed version available at Materials 2019, 12, 382; doi:10.3390/ma12030382

2.3. Nanoporous Networks

Two-dimensional nanoporous networks consist in self-assembly monolayers with a porous pattern which are able to host small molecules. The inclusion of guest molecules is dependent on the size or shape of pore (physical inclusion) or on the molecular recognition (chemical inclusion). The porous array can be modified for specific purposes using rational molecular design. Two methodologies are available for fabrication of nanoporous surfaces depending on the types of building blocks: intrinsic and extrinsic.[28,29]. Nanoporous monolayers developed with intrinsic building blocks are founded on macrocyclic molecular structures that are pre-designed with a hollow centre and synthesised beforehand and with specific physical and chemical characteristics. Upon deposition, they retain the designed properties for each intrinsic nanopore, e.g. pore size. Circular molecular structures that can be used as intrinsic building blocks can occur in nature, e.g. proteins and protein complexes, or be specifically synthesised with a hollow centre, as crown ethers, porphyrins and phthalocyanines.
Nanoporous monolayers developed with extrinsic building blocks depend on the self-assembly of acyclic molecules that together form extrinsic pores. The most used extrinsic building blocks are as trimesic acid (TMA)[30,31], dehydrobenzo[12]annulene (DBA)[32–36] and decycanooligophenylenes[37,38]. They form hexagonal nanopores in which pore size may be modulated by changing the chemical composition of each building block[28–30,34]. These are the most attractive systems, since it is possible to modify the pore properties using specific building blocks to obtain a desired purpose. The fabrication of flat well-defined nanoporous surfaces is not trivial and the deposition conditions, tailored to a goal, must be studied and met. To ensure that the deposited molecules retain a specific packing arrangement avoiding pore hinderance or self-assembly of flat-lying monolayers it is important to know the interactions between molecules and surface. Table 1 resumes the main interactions of these extrinsic building blocks that were analyzed in nanoporous self-assembled networks[39].

Table 1. Table resuming the three groups of building blocks used to form nanoporous self-assembled monolayers

Nanoporous self-assembled networks			
Chemical bonds between building blocks	**Building block**	**Range of cavity diameter**	**Refs**
Hydrogen bonds	TMA	1-2.8 nm	[30,31]
Van der Walls interactions	DBA	1.6-4.7 nm	[32,33,35,40]
Metal-Ligand coordination bonds	Decycanooligophenylene	4.2-6.7 nm	[37,38]

The solvent can play an important role in the formation of nanoporous networks. Lackinger *et al.* [30,31] demonstrated how the solvent can induce different types of nanopores. The authors reported the formation of a self-assembled nanoporous monolayer using TMA as an extrinsic molecular building block that forms two polymorphs influenced by the presence of alkanoic acids that were used as solvent. They analyzed the influence of alkyl chain length of the alkanoic acids, from butyric to nonanoic, analyzing what happens to the molecular arrangement of TMA molecules in the presence of the different solvents. They observed that the solubility decreases in function of the increase in the alkyl chains and a "flower" patterned was observed for shorter acids (butyric to haxanoic acid) while a "chickenwire" was obtained for octanoic and nonanoic acids. The obtained porous have the same dimension for both structures (about 1 nm) but the center-to-center distance between pores is 1.7 nm for the "chickenwire" and 2.5 nm for the flower arrangement.
A second class of extrinsic building blocks are alkyl-/alkoxy-hexadehydrotribenzo[12]annulene (DBA) molecules which have important properties that allow the formation of reproducible nanoporous [34–36,41]. They have alkyl chains as substitutes which allows the interdigitation of chains between neighbour DBA molecules. Interdigitation is dependent on chain length, type of solvent, concentration of DBA molecules and temperature[35,41]. By controlling these parameters, the authors were able

Preprints (www.preprints.org) | NOT PEER-REVIEWED | Posted: 24 December 2018 doi:10.20944/preprints201812.0290.v1

Peer-reviewed version available at Materials 2019, 12, 382; doi:10.3390/ma12030382

to design specific features for the resulting nanopore network, such as, the nanopore diameter and the unit cell which represents the array. The stabilization of the honeycomb array can be ensured by introducing solvent molecules which have an high affinity with the substrate and that coadsorb with the DBA molecules ("template-induced" method) or controlling the concentration of molecules in solution ("concentration-in-control method").

Interdigitation is dependent on chain length, type of solvent, concentration of DBA molecules and temperature[35,41]. By controlling these parameters, the authors were able to design specific features for the resulting nanopore network, such as, the nanopore diameter and chemical modifications at the core surface. The authors reported that a diluted solution of DBA molecules with shorter alkyl chains in a good solvent and at high temperature tend to adopt a more densely packed structure. Additionally, at high concentration of DBA molecules in 1,2,4-trichlorobenzene (TCB), porous networks were only achieved for DBA-OC10 and DBA-OC12, contrariwise DBA-OC14 and DBA-OC16 yielded non porous monolayers. DBA-OCns nanoporous networks can reach pore diameters from 1.6 nm to 4.7 nm, depending on the length of the alkyl chains.

A functionalization of the alkyl chains of DBA molecules, that can generate distinct nanoporous arrays, allows the modulation of their physical and chemical characteristics, *i.e.* pore size, shape and electrostatic properties. Tahara *et al.*[33] reported on an equally functionalized network built with the ability to tailor nanoporous size reversibly by exposing the array to a specific radiation wavelength. The authors developed a DBA self-assembled nanoporous array, in which the DBA molecules were functionalized with a photoresponsive azobenzene group, to yield azobenzene-functionalized DBA networks. Upon the formation of the array, the azobene group can be stimulated by light to induce a conformational change in the DBA network, uniformly establishing a new nanoporous network. Nanoporous arrays can be also composed of contrasting motifs within the same array, since sections of the array can be functionalized differently, i.e. they are periodically functionalized. The authors achieved this by using non-isotopological DBA molecules.[32] Non-isotopological DBA based arrays, with a honeycomb structure, can be assembled with functionalized and unfunctionalized nanowells, achieving a network array with distinct pore sizes. This was obtained after annealing a monolayer of isophthalic acid units connected by an azonbenzene linker to the alkyl chains on the top of HOPG. Figure 4 shows a STM image of the obtained monolayer at HOPG/ 1,2,4-trichlorobenzene interface which presents an honeycomb structure. It is possible to observe white triangular features that represents the core of the DBA molecule and darker region fulfilled by the interdigitated chains deriving from the DBA cores. Two types of nanoporous are formed and indicated by the blue (larger pores) and white (smaller pores) arrows and they are also represented by the molecular model in Figure 4 (b).

Preprints (www.preprints.org) | NOT PEER-REVIEWED | Posted: 24 December 2018 doi:10.20944/preprints201812.0290.v1

Peer-reviewed version available at Materials 2019, 12, 382; doi:10.3390/ma12030382

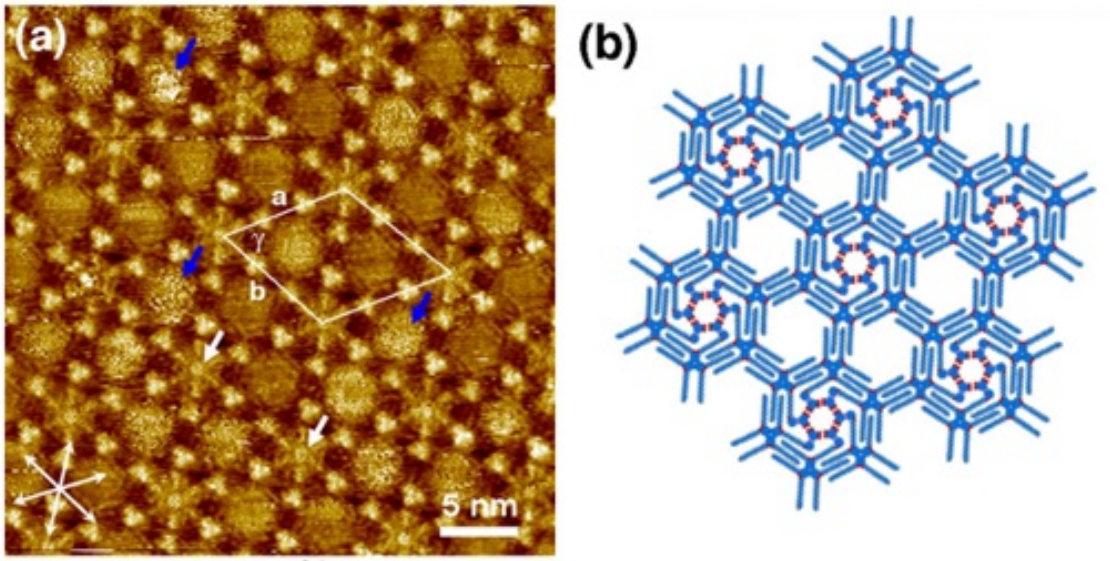

Figure 4. *(a)* STM image of a self-assembled monolayer of DBA functionalized with isophthalic acid linked to the alkyl chains by azobenzene groups. The image shows an honeycomb array characterized by two types of pores: smaller ones indicated by white arrows surronded by the isophthalic units and larger ones indicated by blue arrows involved by the interdigitated alkyl chains. *(b)* molecular model of the DBA monolayer observed in *(a)*. [32]Copyright from 2016 American Chemical Society.)

Dicycanooligophenylenes are another class of building blocks which form isotopological hexagonal packings that are governed by metal-ligand coordination bonds [37,38]. The reported works were not develop at ambient conditions and the authors used UHV conditions to obtain the organized network. In spite of that, these systems can be explored in order to be used at ambient conditions.

The design of nanoporous surfaces has been a challenge due to the several applications of these systems [39]. The inclusion of guest molecules is another important point to be taken into account, since in some cases, their chemical and physical properties are changed after inclusion in the nanoporous network.

2.4. Host-Guest Systems

Host-molecule networks can integrate guest-molecules, which can be single molecules, homoclusters or heteroclusters. Host-guest systems can be used in their simpler form or be chemically modified, thereby allowing modulation and functionality control of interior of each nanopore conferring more versatility to host matrices[28]. The alignment of concepts of rationally designed 2D nanoporous networks and host-guest chemistry is valuable for a diverse range of applications, namely tailored catalysis. For this application, shape and size of each nanoreactor are crucial for binding. Host-guest dedicated requirements are comprised of sensitivity, selectiveness and stimuli-responsiveness upon binding. The nanopore size and shape also require consideration for complementarity. Nevertheless, the challenge in the design and synthesis of host molecules relies, not only on host-guest chemistry, but also on the stability and the characteristics of the host network itself. Lackinger[31] and Griess *et al.*[42] reported that a porous TMA host matrix of 1.3 *nm* average pore size is ideal to accommodate planar and spherical guest molecules of similar sizes (e.g. coronene, sunflower, C60, and triangular nanographene) via van der Walls interactions between substrate and host matrix.

Simple DBA host networks can also be modelled, accommodating different guests, in size by changing the length of the alkyl chains and the concentration of the guest. Balandina *et al.*[43], showed that the length of alkyl chain of the host, the solvent and the concentration of guest molecules influences the equilibrium of the system. Considering Coronene (COR), spherical-like molecule, as a guest, the

Preprints (www.preprints.org) | NOT PEER-REVIEWED | Posted: 24 December 2018 doi:10.20944/preprints201812.0290.v1

Peer-reviewed version available at Materials 2019, 12, 382; doi:10.3390/ma12030382

authors reported that one COR molecule could be fit in a DBA-OC6 nanowell network, while for networks of DBA-OC10, COR is co-adsorbed with solvent molecules. For longer alkyl chains (DBA -OC14 and -OC16) a phase transition on the host structure is induced by an increase of concentration of guest COR molecules, consequently affecting the equilibrium of the incorporation. Furthermore, a different number of integrated guests can be seen when considering triangular nanographene molecules as triangular-like shaped guests for the same DBA-type network. Lei *et al.*[41,44] observed the integration of up to six triangular nanographene molecules, from hereon referred as TNG[28], into different hexagonal porous networks of DBA molecules composed of alkyl chains with chain length ranging from OC10 to OC20.

Figure 5 represents the dependence [remark= É isto que queres dizer?]betweenof the nanopore size and the number of triangular shaped guests. Comparing Figures 5 from *(a)* to *(f)* we notice a linear increase of guest molecules adsorbed as a function of DBA alkyl chain length. Namely, for the DBA-OC20 we observe a total of six TNG molecules neatly packed inside of DBA pore. The respective STM image shows bright triangular domains organized as an hexagonal motif that is commensurate with the DBA pore shape. An exception was observed for the DBA-OC14 (Figure 5 *(c)*) due to a phase transition that occurred only for this case, in which, the TNG molecules were too mobile to be visualized and are described by the authors as "fuzzy features" present in the STM image at the center of each nanowell. Comparing the integration of both guest molecules into the same type of DBA network, gives some insight into the effects of using different guests and their impact on the host-guest system properties. For example, the shape of the guest affected the shape complementarity with the hexagonal nanowells, i.e. being more commensurable, led to generally a higher number of TNG molecules being adsorbed when compared to COR. Also contributing to this effect was the increased affinity of TNG with HOPG, which was also a contributing factor that led to more guests being adsorbed per nanowell.

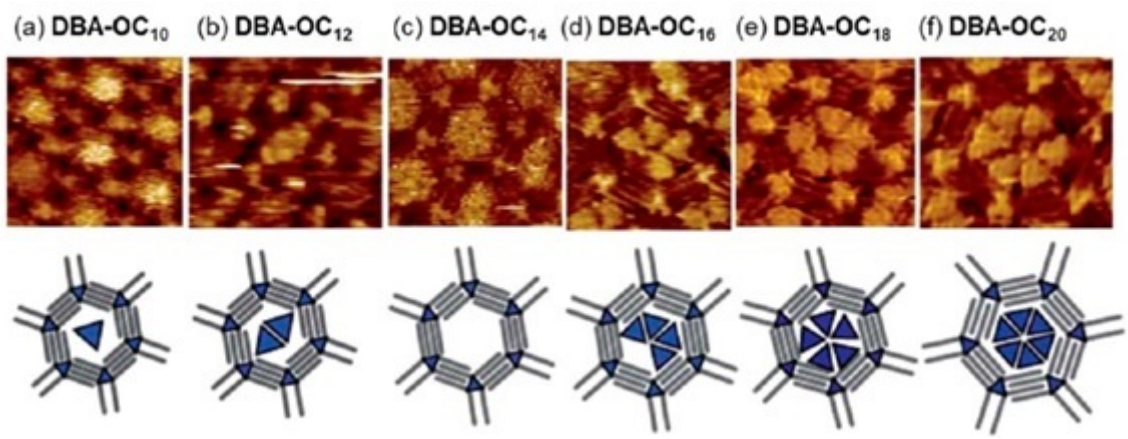

Figure 5. STM images of nanoporous monolayers developed using DBA building blocks with different chain lengths ((a) $DBA-OC10$, (b) $DBA-OC12$, (c) $DBA-OC14$, (d) $DBA-OC16$, (e) $DBA-OC18$, and (f)$DBA-OC20$), and therefore consequently different pore sizes for a host-guest network of $(DBA-OCns)-TNG$. A schematic model of host-guest systems is represented below of each STM image. Different nanowell sizes are able to incorporate different numbers of a guest molecules (TNG). (Reprinted with permission from reference [41]. Copyright 2010 The Royal Society of Chemistry)

Furthermore, a molecule complex can also be integrated as a guest-molecule, which corresponds to more than one guest being adsorbed at the same time as an heteromolecular cluster. Lei *et al.* [45] used a Coronene (COR) and Isophthalic Acid (ISA) complex, in which COR is surrounded by six ISA molecules, as a guest heterocluster to be adsorbed in a DBA network. For this case, the increase of pore size does not correspond to a linear increase of incorporated guests. Observing the STM images of Figure 6 is possible to see the molecular organization of the incorporated cluster represented by

Preprints (www.preprints.org) | NOT PEER-REVIEWED | Posted: 24 December 2018 doi:10.20944/preprints201812.0290.v1

Peer-reviewed version available at Materials 2019, 12, 382; doi:10.3390/ma12030382

the circular brighter domains surrounded by six smaller triangular motifs corresponding to the DBA molecules. The effect of the length alkyl chains was analyzed and only the monolayer composed of DBA-OC10 was able to neatly incorporate the cluster. DBA networks with smaller chain lengths, give smaller pore sizes which do not allow the complex to go inside. For bigger nanopore size the cluster has higher mobility affecting the acuity of STM images acquisition.

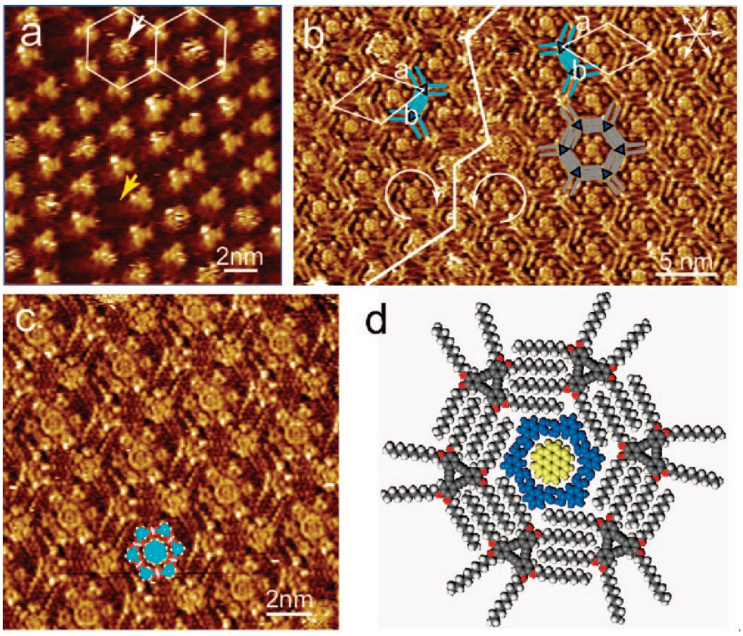

Figure 6. STM images of nanoporous monolayers developed using DBA-OC10 building blocks at the interface of HOPG/1-octanoic acid. The DBA host-network can be visualized with *(a)* and without *(b)* a guest-molecule (an heterocluster of ISA and COR); *(c)* high resolution STM image of *(b)*; *(d)* schematic representation of one host-guest system that is enlarged. (Reprinted with permission from reference [45]. Copyright 2008 The American Chemical Society)

Host-guest chemistry via charge-transfer can also be built using porphyrins at the solid/liquid interface, as reported by Iriani *et al.*[46] using a zinc porphyrin ($DBA - ZnP$). The $DBA - ZnP$ nanoporous network assembled at the HOPG/TBC interface can accommodate C60 fluorene.

Host-guest chemistry can accommodate the catalytic chemical transformations that take place in a nanoreactor. It has the advantage of *tailorability* of physical and chemical properties of each nanoreactor space. The intercalation of organic molecules into molecular suprastructures is promising in the field of fabrication of nanoreactors. Nanoporous network arrays, if properly equipped, as nanoreactors can through chemical interactions capture guest species and reagents for the chemical transformation [28,40,47,48].

3. Molecular machines

A molecular machine is an assembly of molecular elements that have mechanical movement when stimulated by external inputs. Comparing macroscopic with molecular-level machines, both are characterized by the type of energy required to achieve a specific function, and by the manner through which their operation can be monitored. Nevertheless, motion laws are different and consequently the design and manufacturing methods are specific to each scale. The motion of macroscopic machines is described by Newton's equations that cannot be applied to the nanoscale world. With the development of powerful scanning probe microscopies, mainly, with the contribution of STM, the movement of single molecules can be controlled and characterized. All living organisms are composed of thousands of molecular machines, biomolecular machines, that ensure the correct operation of all functions. The way they work can inspire engineers to develop powerful synthetic molecular machines. The concept

Preprints (www.preprints.org) | NOT PEER-REVIEWED | Posted: 24 December 2018 doi:10.20944/preprints201812.0290.v1

Peer-reviewed version available at Materials 2019, 12, 382; doi:10.3390/ma12030382

of molecular machines was promoted by the Nobel Prizes in Chemistry of 2016 [14,49,49–51] who inspired the world of scientists that work in nanotechnology to design molecular machines which move in function of an external stimulus. Ben L. Feringa [52] describes, in his paper, a nanoworld composed of factories with molecular dimensions which are self-repairing, operating with molecular precision and driven by light and chemical energy. Feringa explains that the major difficulty is not to achieve the motion of molecular machines, but in controlling their operation and maintain their stability to ensure directionality. The central part of any molecular machine is the motor, and scientists are focused in developing molecular motors able to operate at room temperature. The following items introduce the most known synthetic molecular machines, molecular switches and motors, build and controlled by STM.

3.1. Molecular Switches

An electronic circuit is managed by a switch which controls current flow. Depending on the complexity of the circuit, the switch can work alone or in combination with multiple switches. A molecular switch is a molecule or a supramolecular system that can exist in two states, ON and OFF, when it is stimulated by an external stimulus. STM has been a commonly employed tool to characterize and to stimulate these structures. The tip is the central part of the experiment and can convert a molecular system into each of the two states in a reversible way. Most of these studies are at solid/liquid interface and allow the characterization of individual electrical properties of both two states, ON and OFF. They can be separated in different categories depending on the stimuli received: electronic, photochromic or mechanically interlocked [53]. The switching properties are dependent on the electrode's composition, the molecular structure and the environment where the experiments are done. The stimuli involved in these experiments are the electrons, which flow from the STM tip, and can consequently induce: desorption and/or dissociation of molecules from a surface, hopping effects, molecular rotation and *in-situ* chemical reactions ([54]).

Most of the experiments occur at low temperatures and at ultra-high vacuum in order to avoid thermally induced effects. However, most of the times, these conditions do not represent the real environment of the molecular device, mainly in biological and organic electronic devices. Marbach *et al.*, induced a conformation of porphyrins presented in a self-assembly monolayer close to room temperature (200 K). STM images of a self-assembly monolayer on Cu(111) showed different conformations of porphyrins in function of the applied tip voltage. Recently, Ferreira and co-workers[55] reported a switchable mechanism of a self-assembly monolayer of porphyrins on HOPG at room temperature induced by STM. Figure 7 shows the dynamics of the porphyrins presented in this monolayer through consecutive STM images acquired in the same region at constant current and at alternate tip potentials of 0.4 and 0.7 V. Figures *(A)* to *(D)* evidentiate an alternate behaviour for each tip potential. Analyzing Figure 7 (E) we can observe two types of porphyrins well distinguished by the apparent height in the respective line profile of Figure 7 (F). The authors attributed these differences to different molecules conformations associated to different pyrrole groups positions. The pyrrole groups of brighter lines are in *trans* conformation and the darker lines correspond to a *cis* conformation. When the tip voltage increases to 0.7 V the *trans* molecules switch to a *cis* conformation and the monolayer becomes homogeneous as it is indicated by the line profile of Figure 7 (F). It was observed that the response of porphyrins to the tip-voltage is reversible and does not cause disorders in the self-assembly monolayer. This work evidences the stability of self-assembly molecular switches at room-temperature and remarks the idea that they are great candidates to connect with other molecules of a complex electronic circuit.

Preprints (www.preprints.org) | NOT PEER-REVIEWED | Posted: 24 December 2018 doi:10.20944/preprints201812.0290.v1

Peer-reviewed version available at Materials 2019, 12, 382; doi:10.3390/ma12030382

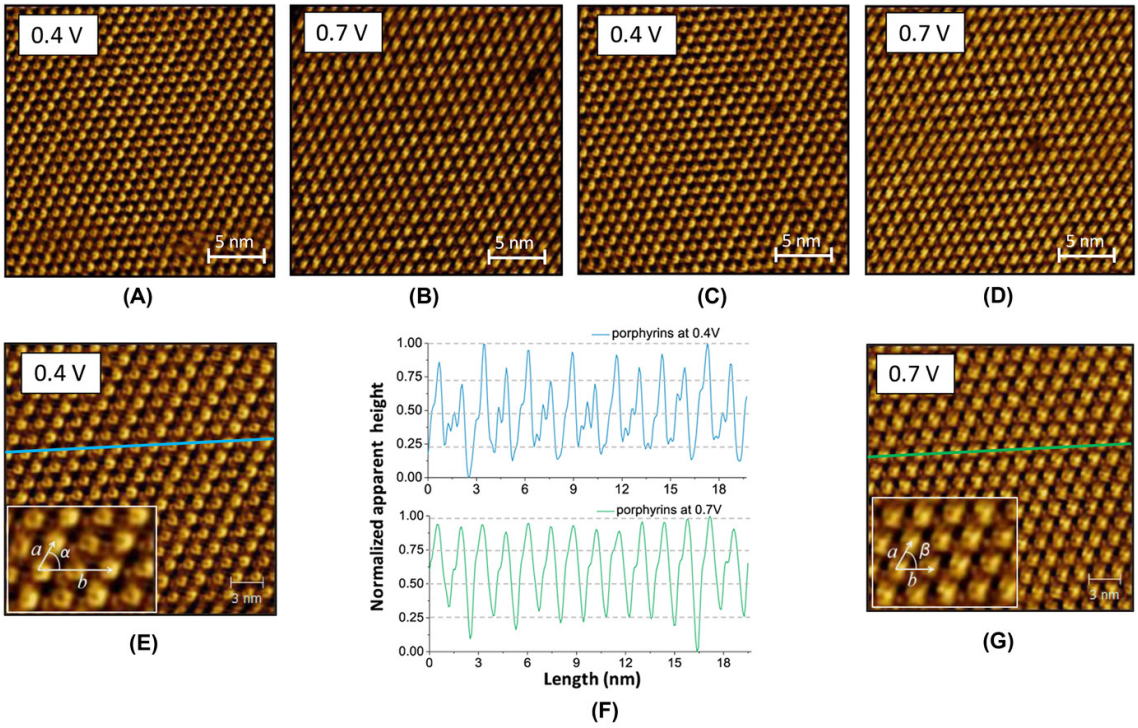

Figure 7. (A-D) Sequential STM images of ZnOEP monolayer at tetradecane/HOPG interface revealing conformational changes upon application of stimuli. (E) the blue line and (G) the green line acquired from the STM images are represented (F) by profile lines in normalized apparent height maps indicating the differences between heights in accordance to different molecular conformations. (Reprinted with permission from reference [55]. Copyright 2018 Authors and Royal Microscopical Society)

3.2. Molecular Motors

Movement is essential to life, may it be in the form of transport, translocation, contraction or others, since ultimately biological systems rely directly or indirectly on movement. It is for this aspect, that molecular motors, which have ability of powering movement, are intrinsic to nature. Molecular motors are commonly seen in nature, adenosine triphosphate synthase, myosin, kinesin and dynein. These are motor proteins that convert chemical energy to attain directional movement. Inspired by these biological machines, molecules and molecular complexes that can be assembled to form rotors and motors have been designed and fabricated at the nanoscale to simulate biological functions such as movement. A motor is commonly defined as an energy converter system, *i.e.* a system capable of converting one type of energy - e.g. electromagnetic, chemical, electrical - into kinetic energy. Specifically, a rotary motor is capable of converting this energy into unidirectional rotary movement in a controlled manner. Rotary molecular motors are commonly composed of three components: the rotor, the axle and the stator[14,49,56–59]. Research on rotary molecules has been developed almost over the last two decades, with increasing focus on systems anchored to solid surfaces. In 2005, Feringa and co-workers[56] envisioned that unidirectional rotors could be assembled as anchored molecular motors. The motors, developed in solution and anchored to gold nanoparticles, were composed of a helical alkene as a rotor, a carbon-carbon double bond as axle and two thiol-functionalised legs that anchor to a gold stator. The authors introduce here a system in which conformational molecular changes on the rotor are light driven and consequently induce unidirectional (360°) rotation movement. This publication propelled further studies withing the field in which movement was brought upon by different stimuli and in other mediums (e.g. solution, vacuum and at interfaces), *i.e.*, fabrication of rotors at the nanoscale could be tuned using i) radiation, ii) electric fields induced by the STM tips and even iii) oxidation-reduction reactions[60,61].

Preprints (www.preprints.org) | NOT PEER-REVIEWED | Posted: 24 December 2018 doi:10.20944/preprints201812.0290.v1

Peer-reviewed version available at Materials 2019, 12, 382; doi:10.3390/ma12030382

In the field of molecular motors, focus has been given to studies at room-temperature and some important contributions have been published with dynamic molecular systems in these conditions [61–65]. A recent work[63] reports a walking molecule moving freely at room-temperature between two stationary points. The authors analyzed the movements of a divalent bis(imidazolyl) molecule, that they called a "walker", which moves with an inchworm mechanism by attachment and detachment cycles between two immobilized cobalt porphyrins. Figure 8 shows a schematic representation of this system with a walker moving on an anisotropic Cu (110) surface. Density functional theory (DFT) calculations (Figure 8 (iii) and (iv)) demonstrated that the imidazole adopts a "horseshoe conformation" characterized by the phenyl ring which is pulled upwards and the two imidazolyl groups that are in contact with surface, work as the feet of molecule. These imidazolyl groups are responsible for the movement through attachments and detachments. The walker moves freely through two opposite porphyrins. The system is thermally activated at room temperature and authors suggest that it is a good candidate for molecular machines controlled by light or electrical pulses.

Preprints (www.preprints.org) | NOT PEER-REVIEWED | Posted: 24 December 2018 doi:10.20944/preprints201812.0290.v1

Peer-reviewed version available at Materials 2019, 12, 382; doi:10.3390/ma12030382

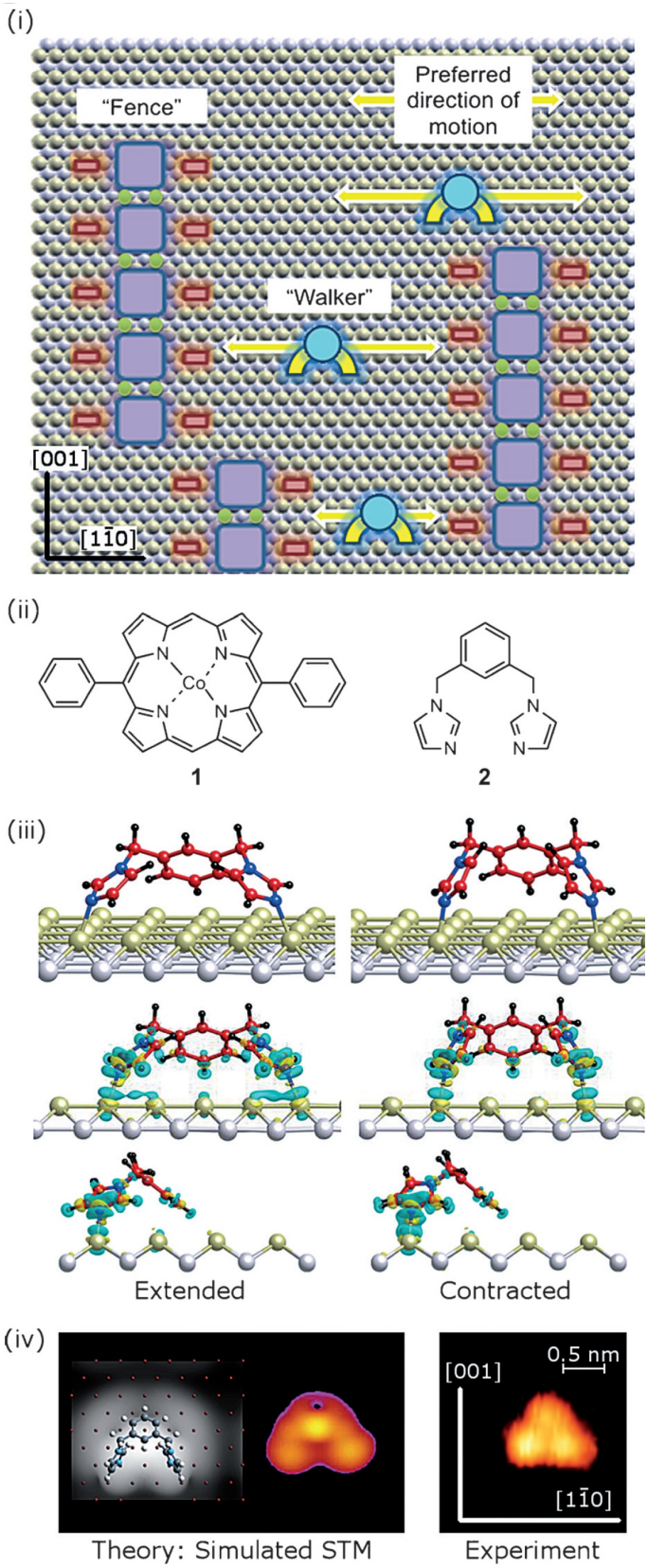

Figure 8. (i) Schematic representation of a walking molecule - walker, which moves between two immobilized fences. The walker is a divalent bis(imidazolyl) molecule and the fence is a cobalt porphyrin represented in (ii). The walker moves by attachment and detachment cycles between two fences. As represented by DFT simulations in (iii) and (iv) and the respective experimental STM image (iv). Reprinted with permission from reference [63]. Copyright 2015 WILEY-VCH Verlag GmbH & Co. KGaA, Weinheim.

Preprints (www.preprints.org) | NOT PEER-REVIEWED | Posted: 24 December 2018 doi:10.20944/preprints201812.0290.v1

Peer-reviewed version available at Materials 2019, 12, 382; doi:10.3390/ma12030382

The development of molecular motors needs to overcome certain limitations. Apart from their stability at room temperature, the focus is to develop fast machines able to "walk" over longer distances. To explore how fast and how far a nanomotor can travel, the first world-wide nanocar competing event took place using the STM to control and monitor the results [66–68]. The competition came to pass in the CEMES-CNRS centre, in Toulouse, with six competing nanocars, over the span of two days and a half. The STM tip was employed as an external stimulus to drive the cars by applying an electrical voltage. All races were performed under ultrahigh vacuum, at a temperature of 4 K and over gold surface, apart from one which was performed over silver. It was stipulated that each nanocar should perform at least two laps in a 100 nm circuit. The results and details are described by G. Rapenne and C. Joachim in the reference [68]. The winners were Rice–Graz and Basel whose car took 29 hours to run across 1 μm. This can be the most impressive experiment with molecular machines that involved the collaboration of several international research teams. Via these experiments we can improve our understanding on the requirements to design robust molecular machines that can operate over long periods.

4. Molecular Wires

The first definition of a molecular wire (MW) was given by the chemistry nobel prize Jean-Marie Lehn in 1988, that defined this structure as a conductive chain of a molecule or a supramolecule which conducts electrons between two electrodes [69]. The MW is an important piece of a molecular electronic circuit considering that it can connect the single molecule elements. The MWs have been studied by STM, mainly their charge transport characteristics using the tip as the top electrode and the substrate as the bottom electrode. The tip measures the electron flow between both electrodes and gives an individual electrical measure of the wire. The charge transport depends on the interactions between the molecular or supramolecular system and electrodes. All existing methods to measure individual properties have limitations and it is still a challenge to establish a method that gives real information about charge transport of MWs. The most used techniques are current-sensing atomic force microscopy (CSAFM) and STM break junctions (STM BJ). Both techniques require physical contact between tip and MW. However, most of the time, the size of tip that is used in CSAFM is greater when compared to the molecule size and it is impossible to measure an individual MW without the influence of neighbouring molecular systems. In the STM BJ the existing chemical contact between tip and molecule provides a great advantage. [70] A recent example of MWs that work as molecular switches under aqueous environments shows how it is possible to tune a single-molecule-based pH sensor electrically by STM break junctions. [71] The authors measured the electrical properties of $4,4'$-vinylenedipyridine (44VDP) using Ni contacts and in a solution with 0.05 M of Na_2SO_4. They monitored redox reactions at single molecule level controlling the pH of environment and the electrochemical potential. They observed a dependence of electrical properties on the pH of solution. The conductance switching of Ni | 44VDP | Ni molecular junctions is due to redox reactions which occur in the terminal groups and that changes the conductance. These molecular systems can be used as a pH-sensitive switch and the pH at which occurs the switch event can be tuned using a gate voltage. This is an example on how the STM can control molecular conductance trough the management of pH and bias voltage.

The conductance measurements at single level are experimentally challenging and each systems need specific experimental protocols. The STM BJ experiments seem to be perfect taking into account that the electrodes make a contact with the molecular systems. However, it is difficult to know how this affects the structure and vibrational properties of the structure that is being analyzed.

Scanning Tunneling Spectroscopy (STS) is another technique to measure electrical properties of individual wires. Its main limitation is the non contact between tip and MW that compromisses the accuracy of measurements. However, STS can be supported by STM images that can be acquired simultaneously with current measurements. This allows the precise localization of MWs ensuring that the tip is analyzing the desired structure. The most reported works about MWs are related to

Preprints (www.preprints.org) | NOT PEER-REVIEWED | Posted: 24 December 2018 doi:10.20944/preprints201812.0290.v1

Peer-reviewed version available at Materials 2019, 12, 382; doi:10.3390/ma12030382

supramolecular structures previously synthesized in laboratory or locally synthesized at high vacuum conditions [72] .

A recent work[7] shows how it is possible to use a combination of STM at solid/liquid interface and STS to built a MW and to measure its individual electrical properties at room temperature. Vertical MWs with 14 nm of length were build using a stepwise method from 23 molecules added one by one. Zinc (II) octaethylporphyrins (ZnOEP) assembled on HOPG were bonded by 4,4′-bipyridine (BP) via coordination of the nitrogen atom to the zinc atom. The ZnOEP and BP are two building blocks which were added sequentially until achieving the desired structure. These experiments were made at HOPG/tetradecane interface imaging each step with STM to control the formation of each molecular bond. Figure 9 shows a schematic representation of MWs composed of 4, 9 and 23 building blocks and the respective STM images. Observing the image of Figure 9 *a)* it is possible to observe, at high resolution, the 4th monolayer with a defect that allows the visualization of the monolayer immediately below. Each brighter spot corresponds to the top of a MW composed of 4 molecules, covalently linked: ZnOEP/BP/ZnOEP/BP. The respective line profiles highlight the presence of the last molecule (BP) and the ZnOEP before that. The authors reported, in this work, the STM images of all steps maintaining the resolution until last monolayer, as it is possible to see in Figure 9 *c)*. The electric characteristics of individual wires were also quantified by authors using STS during the scanning of each monolayer.

Preprints (www.preprints.org) | NOT PEER-REVIEWED | Posted: 24 December 2018 doi:10.20944/preprints201812.0290.v1

Peer-reviewed version available at Materials 2019, 12, 382; doi:10.3390/ma12030382

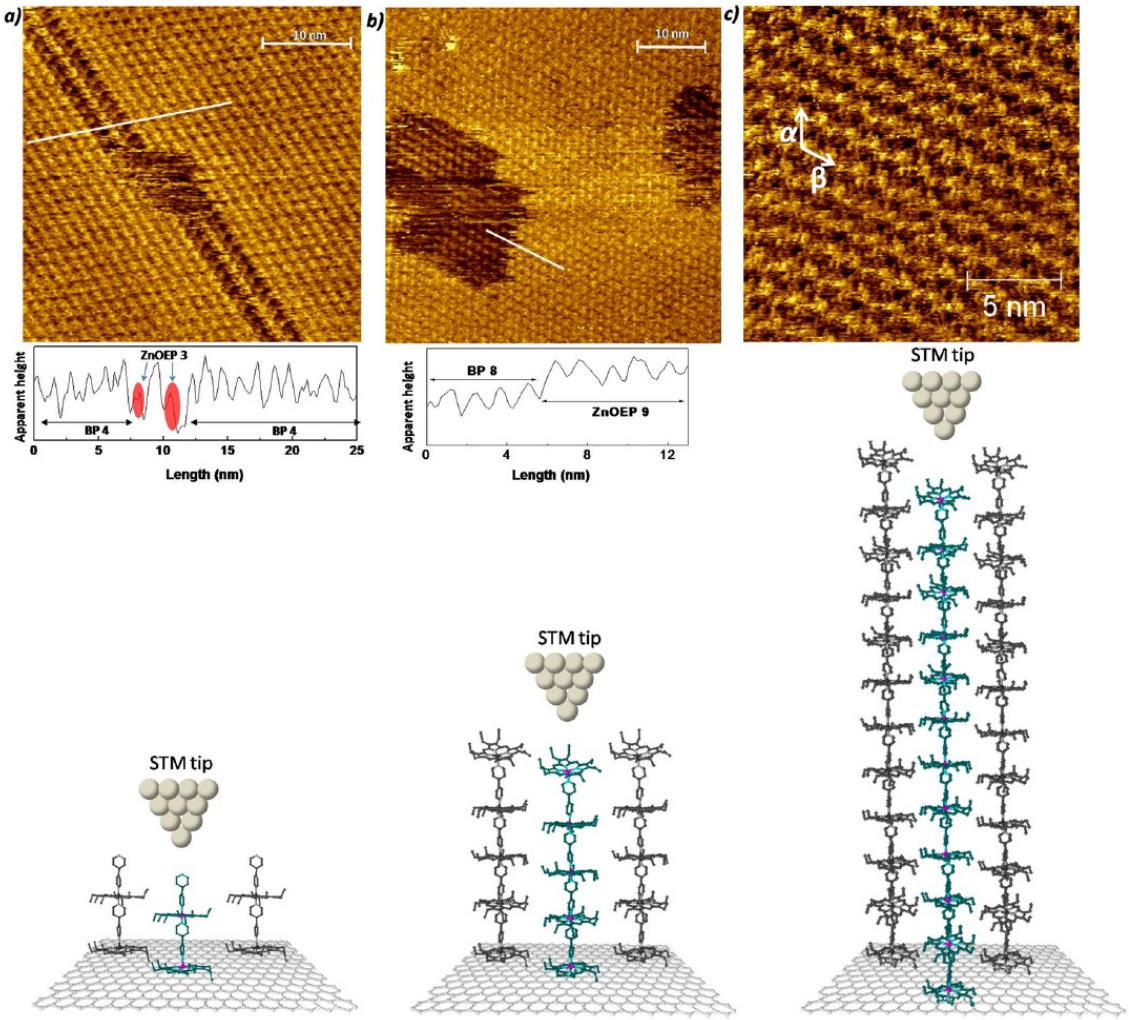

Figure 9. STM images of bipyridine monolayers assembled in intercalated structures with ZnOEP: (a) represents the fourth self-assembled monolayer (BP) developed over the third layer (darker regions - ZnOEP); (b) the ninth layer (ZnOEP) developed over the eighth layer (darker regions – BP), with corresponding line profiles evidencing the height differences in the monolayer; and (c) the twenty-third layer (ZnOEP). The schematics immediately bellow the STM images are models of the BP-ZnOEP alternative self-assembly layer-by-layer. (Reprinted with permission from reference[7]. Copyright 2014 American Chemical Society)

The image allows positioning and placing the tip on the top of a single wire. At this moment, the individual current was measured by the application of a bias voltage between tip and substrate. The characterization of conduction mechanisms was identified analyzing the evolution of MWs electrical resistance as function of the molecular length associating a tunneling mechanism for shorter wires with 4-5 nm and a hopping mechanism for longer wires. This work can act as a model to built similar supramolecular structures synthesized *in-situ*. Each step can be controlled by images with molecular resolution while at the same time the individual electric transport can be measured.
The described stepwise method allows the design of MWs more efficiently, changing for example the building blocks in order to obtain more conductive wires.

5. Future perspective

One of the questions that we make when we look at the developments of unimolecular devices is: when will they be integrated in electronic circuits? The answer can be supported by the fast evolution in this research field covering a wide range of applications and prototypes which are already working

Preprints (www.preprints.org) | NOT PEER-REVIEWED | Posted: 24 December 2018 doi:10.20944/preprints201812.0290.v1

Peer-reviewed version available at Materials 2019, 12, 382; doi:10.3390/ma12030382

[73–78] Organic sensors, organic solar cells, organic transistors, organic light emitting diodes are no longer future projects and they are already existing in our days. The breakthrough for the development of organic devices is to develop smart devices able to replace all silicon semiconductor components. The trend is to learn with biological systems [79–85].

In order to develop functional devices it is important to understand how biological machines work and mimic their mechanisms. At first instance, this could be an easy task considering that we have 23 building blocks in nature corresponding to the amino acids. However, most of the mechanisms of biological systems still remain unknown. The focus has been centered in studying individual biological molecules [83,84].

STM has been a fundamental tool to study bio systems in aqueous environments [86]. The characterization of electrical properties of biomolecules can help us to design bioelectronic devices. Charge transport characteristics of redox proteins have been studied in nanodevices. For example, Cu-azurin was analyzed in microscale solid-state devices [87–89]. Namely, single-protein junctions of Cu-azurin were performed with STM and showed that it is possible to manipulate conformations preserving the protein structure[84].

Besides the interest in biological systems, there are other challenges to overcome:

- to create unimolecular systems stable at room temperatures;
- to develop encapsulation methods while maintaining the integrity of the organic device.

A recent work, shows how it is possible to built flexible MWs stable at room temperature[90]. MWs with approximately 4 nm of length composed of disulfanyl carbon-bridged oligo-(phenylenevinylene) ($COPV_6(SH)_2$) maintained their electronic characteristics at room temperature during 3 months and an high tolerance for low and high temperatures. The authors explained that this behaviour is due to the structural characteristics of $COPV_6$ which is a rigid and planar molecular system composed of a conjugated wire which is protected by an insulating sheath. Consequently the electron flow is stable and does not suffer influences from other neighbouring molecular systems. This can be the departure point to optimize these systems and implement them in electronic circuits.

The stability of an organic device also depends on the encapsulation and this research is still at the beginning. All devices need to be encapsulated to be protected from corrosion and to avoid degradation in the presence of air. L. Moro *et al.* published a recent article in which gives an overview of the requirements to develop encapsulation methods for organic devices [91]. This is a research field which needs a greater dedication and work in order to accomplish the fast development of devices.

At the moment, the main concern of scientists is to integrate the single molecule device in a final electronic circuit. To achieve this goal it is necessary to overcome important constraints: long-term stability, biocompatibility and environment effects.

Funding: The work was supported by Fundação para a Ciência e a Tecnologia by the project UIDEEA500082013

Acknowledgments: The authors acknowledge the financial support from Fundação para a Ciência e a Tecnologia by the project UID/EEA/50008/2013

References

1. Inácio, P.; Mestre, A.G.; Medeiros, M.C.R.; Asgarifar, S.; Elamine, Y.; Canudo, J.; Santos, J.; Bragança, J.; Morgado, J.; Biscarini, F.; Gomes, H. Bioelectrical Signal Detection Using Conducting Polymer Electrodes and the Displacement Current Method. *IEEE Sensors Journal* **2017**, *17*, 3961–3966. doi:10.1109/JSEN.2017.2703834.
2. Krishnamoorthy, P.K.; Ferreira, B.F.; Gomes, C.S.B.; Vila-Viçosa, D.; Charas, A.; Morgado, J.; Calhorda, M.; Maçanita, A.; Gomes, P. Violet-Blue emitting 2-(N-Alkylimino)pyrrolyl Organoboranes: Synthesis, Structure and Luminescent Properties. *Dyes and Pigments* **2017**, *140*, 520– 532. doi:10.1016/j.dyepig.2016.11.017.

Preprints (www.preprints.org) | NOT PEER-REVIEWED | Posted: 24 December 2018 doi:10.20944/preprints201812.0290.v1

Peer-reviewed version available at Materials 2019, 12, 382; doi:10.3390/ma12030382

3. Meng, L.; Zhang, Y.; Wan, X.; Li, C.; Zhang, X.; Wang, Y.; Ke, X.; Xiao, Z.; Ding, L.; Xia, R.; Yip, H.L.; Cao, Y.; Chen, Y. Organic and solution-processed tandem solar cells with 17.3% efficiency. *Science* **2018**, *361*. doi:10.1126/science.aat2612.
4. Farinhas, J.; Oliveira, R.; Hansson, R.H.; Ericsson, L.K.E.E.; Moons, E.M.; Morgado, J.; Charas, A. Efficient ternary organic solar cells based on immiscible blends. *Organic Electronics* **2017**, *41*, 130–136. doi:10.1016/j.orgel.2016.12.009.
5. Afonso, M.; Morgado, J.; Alcácer, L. Inkjet printed organic electrochemical transistors with highly conducting polymer electrolytes. *Journal Applied Physics* **2016**, *120*, 1–6. doi:10.1063/1.4966651.
6. Ferreira, Q.; Alcácer, L.; Morgado, J. Stepwise preparation and characterization of molecular wires made of zinc octaethylporphyrin complexes bridged by 4, 4-bipyridine on HOPG. *Nanotechnology* **2011**, *22*, 435604.
7. Ferreira, Q.; Braganca, A.M.; Alcacer, L.; Morgado, J. Conductance of well-defined porphyrin self-assembled molecular wires up to 14 nm in length. *The Journal of Physical Chemistry C* **2014**, *118*, 7229–7234.
8. K.E., D. *Engines of creation, The coming Era of Nanotechnology*; Springe28Anchor Press,r: New York, 1986.
9. Pedersen, C.J. The discovery of crown ethers (Noble Lecture). *Angewandte Chemie International Edition in English* **1988**, *27*, 1021–1027.
10. Cram, D.J. The design of molecular hosts, guests, and their complexes (Nobel lecture). *Angewandte Chemie International Edition in English* **1988**, *27*, 1009–1020.
11. Lehn, J.M. Supramolecular chemistry—scope and perspectives molecules, supermolecules, and molecular devices (Nobel Lecture). *Angewandte Chemie International Edition in English* **1988**, *27*, 89–112.
12. Sauvage, J.P. From chemical topology to molecular machines (Nobel lecture). *Angewandte Chemie International Edition* **2017**, *56*, 11080–11093.
13. Stoddart, J.F. Mechanically interlocked molecules (MIMs)—Molecular shuttles, switches, and machines (Nobel Lecture). *Angewandte Chemie International Edition* **2017**, *56*, 11094–11125.
14. Feringa, B.L. The art of building small: From molecular switches to motors (Nobel lecture). *Angewandte Chemie International Edition* **2017**, *56*, 11060–11078.
15. Otsuki, J.; Seki, E.; Taguchi, T.; Asakawa, M.; Miyake, K. STM observation of labile axial ligands to zinc porphyrin at liquid/solid interface. *Chemistry Letters* **2007**, *36*, 740–741.
16. Ferreira, Q.; Bragança, A.; Moura, N.; Faustino, M.; Alcácer, L.; Morgado, J. Dynamics of porphyrin adsorption on highly oriented pyrolytic graphite monitored by scanning tunnelling microscopy at the liquid/solid interface. *Applied Surface Science* **2013**, *273*, 220–225.
17. Uemura, S.; Tanoue, R.; Yilmaz, N.; Ohira, A.; Kunitake, M. Molecular dynamics in two-dimensional supramolecular systems observed by STM. *Materials* **2010**, *3*, 4252–4276.
18. Samorí, P.; Müllen, K.; Rabe, J.P. Molecular-Scale Tracking of the Self-Healing of Polycrystalline Monolayers at the Solid–Liquid Interface. *Advanced Materials* **2004**, *16*, 1761–1765.
19. Palma, C.A.; Bonini, M.; Breiner, T.; Samorì, P. Supramolecular Crystal Engineering at the Solid–Liquid Interface from First Principles: Toward Unraveling the Thermodynamics of 2D Self-Assembly. *Advanced Materials* **2009**, *21*, 1383–1386.
20. Kim, K.; Plass, K.E.; Matzger, A.J. Kinetic and thermodynamic forms of a two-dimensional crystal. *Langmuir* **2003**, *19*, 7149–7152.
21. Lei, S.; Tahara, K.; De Schryver, F.C.; Van der Auweraer, M.; Tobe, Y.; De Feyter, S. One building block, two different supramolecular surface-confined patterns: concentration in control at the solid–liquid interface. *Angewandte Chemie International Edition* **2008**, *47*, 2964–2968.
22. Gesquière, A.; Abdel-Mottaleb, M.M.; De Feyter, S.; De Schryver, F.C.; Sieffert, M.; Müllen, K.; Calderone, A.; Lazzaroni, R.; Brédas, J.L. Dynamics in Physisorbed Monolayers of 5-Alkoxy-isophthalic Acid Derivatives at the Liquid/Solid Interface Investigated by Scanning Tunneling Microscopy. *Chemistry–A European Journal* **2000**, *6*, 3739–3746.
23. Sirtl, T.; Song, W.; Eder, G.; Neogi, S.; Schmittel, M.; Heckl, W.M.; Lackinger, M. Solvent-Dependent Stabilization of Metastable Monolayer Polymorphs at the Liquid–Solid Interface. *ACS Nano* **2013**, *7*, 6711–6718, [https://doi.org/10.1021/nn4014577]. PMID: 23875955, doi:10.1021/nn4014577.
24. Jahanbekam, A.; Vorpahl, S.; Mazur, U.; Hipps, K. Temperature stability of three commensurate surface structures of coronene adsorbed on Au (111) from heptanoic acid in the 0 to 60 C range. *The Journal of Physical Chemistry C* **2013**, *117*, 2914–2919.

Preprints (www.preprints.org) | NOT PEER-REVIEWED | Posted: 24 December 2018 doi:10.20944/preprints201812.0290.v1

Peer-reviewed version available at Materials 2019, 12, 382; doi:10.3390/ma12030382

25. Dienstmaier, J.F.; Mahata, K.; Walch, H.; Heckl, W.M.; Schmittel, M.; Lackinger, M. On the Scalability of Supramolecular Networks- High Packing Density vs Optimized Hydrogen Bonds in Tricarboxylic Acid Monolayers. *Langmuir* **2010**, *26*, 10708–10716.
26. Zhang, R.; Yan, Q.; Shen, Y.; Gan, L.; Zeng, Q.d.; Zhao, D.; Wang, C. Conformational polymorphism of multimeric perylene derivatives observed by using scanning tunneling microscopy. *CrystEngComm* **2011**, *13*, 5566–5570.
27. Visser, J.; Katsonis, N.; Vicario, J.; Feringa, B.L. Two-dimensional molecular patterning by surface-enhanced zn-porphyrin coordination. *Langmuir* **2009**, *25*, 5980–5985.
28. Iritani, K.; Tahara, K.; De Feyter, S.; Tobe, Y. Host–guest chemistry in integrated porous space formed by molecular self-assembly at liquid–solid interfaces. *Langmuir* **2017**, *33*, 4601–4618.
29. Kudernac, T.; Lei, S.; Elemans, J.A.; De Feyter, S. Two-dimensional supramolecular self-assembly: nanoporous networks on surfaces. *Chemical Society Reviews* **2009**, *38*, 402–421.
30. Lackinger, M.; Griessl, S.; Heckl, W.M.; Hietschold, M.; Flynn, G.W. Self-assembly of trimesic acid at the liquid- solid interface a study of solvent-induced polymorphism. *Langmuir* **2005**, *21*, 4984–4988.
31. Lackinger, M.; Heckl, W.M. Carboxylic acids: versatile building blocks and mediators for two-dimensional supramolecular self-assembly. *Langmuir* **2009**, *25*, 11307–11321.
32. Tahara, K.; Nakatani, K.; Iritani, K.; De Feyter, S.; Tobe, Y. Periodic Functionalization of Surface-Confined Pores in a Two-Dimensional Porous Network Using a Tailored Molecular Building Block. *ACS nano* **2016**, *10*, 2113–2120.
33. Tahara, K.; Inukai, K.; Adisoejoso, J.; Yamaga, H.; Balandina, T.; Blunt, M.O.; De Feyter, S.; Tobe, Y. Tailoring Surface-Confined Nanopores with Photoresponsive Groups. *Angewandte Chemie International Edition* **2013**, *52*, 8373–8376.
34. Tahara, K.; Furukawa, S.; Uji-i, H.; Uchino, T.; Ichikawa, T.; Zhang, J.; Mamdouh, W.; Sonoda, M.; De Schryver, F.C.; De Feyter, S.; others. Two-dimensional porous molecular networks of dehydrobenzo [12] annulene derivatives via alkyl chain interdigitation. *Journal of the American Chemical Society* **2006**, *128*, 16613–16625.
35. Tahara, K.; Lei, S.; Adisoejoso, J.; De Feyter, S.; Tobe, Y. Supramolecular surface-confined architectures created by self-assembly of triangular phenylene–ethynylene macrocycles via van der Waals interaction. *Chemical Communications* **2010**, *46*, 8507–8525.
36. Tahara, K.; Adisoejoso, J.; Inukai, K.; Lei, S.; Noguchi, A.; Li, B.; Vanderlinden, W.; De Feyter, S.; Tobe, Y. Harnessing by a diacetylene unit: a molecular design for porous two-dimensional network formation at the liquid/solid interface. *Chemical Communications* **2014**, *50*, 2831–2833.
37. Schlickum, U.; Decker, R.; Klappenberger, F.; Zoppellaro, G.; Klyatskaya, S.; Ruben, M.; Silanes, I.; Arnau, A.; Kern, K.; Brune, H.; Barth, J.V. Metal-Organic Honeycomb Nanomeshes with Tunable Cavity Size. *Nano Letters* **2007**, *7*, 3813–3817, [https://doi.org/10.1021/nl072466m]. PMID: 18020476, doi:10.1021/nl072466m.
38. Kühne, D.; Klappenberger, F.; Decker, R.; Schlickum, U.; Brune, H.; Klyatskaya, S.; Ruben, M.; Barth, J.V. High-Quality 2D Metal-Organic Coordination Network Providing Giant Cavities within Mesoscale Domains. *Journal of the American Chemical Society* **2009**, *131*, 3881–3883, [https://doi.org/10.1021/ja809946z]. PMID: 19256496, doi:10.1021/ja809946z.
39. Iritani, K.; Tahara, K.; De Feyter, S.; Tobe, Y. Host–Guest Chemistry in Integrated Porous Space Formed by Molecular Self-Assembly at Liquid–Solid Interfaces. *Langmuir* **2017**, *33*, 4601–4618, [https://doi.org/10.1021/acs.langmuir.7b00083]. PMID: 28206764, doi:10.1021/acs.langmuir.7b00083.
40. Teyssandier, J.; De Feyter, S.; Mali, K.S. Host–guest chemistry in two-dimensional supramolecular networks. *Chemical Communications* **2016**, *52*, 11465–11487.
41. Lei, S.; Tahara, K.; Adisoejoso, J.; Balandina, T.; Tobe, Y.; De Feyter, S. Towards two-dimensional nanoporous networks: crystal engineering at the solid–liquid interface. *CrystEngComm* **2010**, *12*, 3369–3381.
42. Griessl, S.J.; Lackinger, M.; Jamitzky, F.; Markert, T.; Hietschold, M.; Heckl, W.M. Incorporation and manipulation of coronene in an organic template structure. *Langmuir* **2004**, *20*, 9403–9407.
43. Balandina, T.; Tahara, K.; Sandig, N.; Blunt, M.O.; Adisoejoso, J.; Lei, S.; Zerbetto, F.; Tobe, Y.; De Feyter, S. Role of Substrate in Directing the Self-Assembly of Multicomponent Supramolecular Networks at the Liquid–Solid Interface. *ACS nano* **2012**, *6*, 8381–8389.

Preprints (www.preprints.org) | NOT PEER-REVIEWED | Posted: 24 December 2018 doi:10.20944/preprints201812.0290.v1

Peer-reviewed version available at Materials 2019, 12, 382; doi:10.3390/ma12030382

44. Lei, S.; Tahara, K.; Feng, X.; Furukawa, S.; De Schryver, F.C.; Müllen, K.; Tobe, Y.; De Feyter, S. Molecular clusters in two-dimensional surface-confined nanoporous molecular networks: Structure, rigidity, and dynamics. *Journal of the American Chemical Society* **2008**, *130*, 7119–7129.
45. Lei, S.; Surin, M.; Tahara, K.; Adisoejoso, J.; Lazzaroni, R.; Tobe, Y.; Feyter, S.D. Programmable hierarchical three-component 2D assembly at a liquid- solid interface: recognition, selection, and transformation. *Nano letters* **2008**, *8*, 2541–2546.
46. Iritani, K.; Tahara, K.; Hirose, K.; De Feyter, S.; Tobe, Y. Construction of cyclic arrays of Zn-porphyrin units and their guest binding at the solid–liquid interface. *Chemical Communications* **2016**, *52*, 14419–14422.
47. Bonifazi, D.; Mohnani, S.; Llanes-Pallas, A. Supramolecular chemistry at interfaces: molecular recognition on nanopatterned porous surfaces. *Chemistry–A European Journal* **2009**, *15*, 7004–7025.
48. Fang, Y.; Ghijsens, E.; Ivasenko, O.; Cao, H.; Noguchi, A.; Mali, K.S.; Tahara, K.; Tobe, Y.; De Feyter, S. Dynamic control over supramolecular handedness by selecting chiral induction pathways at the solution–solid interface. *Nature chemistry* **2016**, *8*, 711.
49. Ellis, E.; Moorthy, S.; Chio, W.I.K.; Lee, T.C. Artificial molecular and nanostructures for advanced nanomachinery. *Chemical Communications* **2018**, *54*, 4075–4090.
50. Franken, L.; Wei, Y.; Chen, J.; Boekema, E.J.; Zhao, D.; Stuart, M.C.; Feringa, B.L. Solvent mixing to induce molecular motor aggregation into bowl-shaped particles: underlying mechanism, particle nature and application to control motor behavior. *Journal of the American Chemical Society* **2018**.
51. Klymchenko, A.S.; Sleven, J.; Binnemans, K.; De Feyter, S. Two-dimensional self-assembly and phase behavior of an alkoxylated sandwich-type bisphthalocyanine and its phthalocyanine analogues at the liquid- solid interface. *Langmuir* **2006**, *22*, 723–728.
52. Wesley.; Brown, B.L.; Feringa. Making molecular machines work. *Nature Nanothechnology* **2006**, *1*, 25–35.
53. Pathem, B.K.; Claridge, S.A.; Zheng, Y.B.; Weiss, P.S. Molecular switches and motors on surfaces. *Annual review of physical chemistry* **2013**, *64*, 605–630.
54. Zhang, J.L.; Zhong, J.Q.; Lin, J.D.; Hu, W.P.; Wu, K.; Xu, G.Q.; Wee, A.T.; Chen, W. Towards single molecule switches. *Chemical Society Reviews* **2015**, *44*, 2998–3022.
55. Oliveira, J.; Bragança, A.; Alcácer, L.; Morgado, J.; Figueiredo, M.; BIOUCAS-DIAS, J.; Ferreira, Q. Sparse-coding denoising applied to reversible conformational switching of a porphyrin self-assembled monolayer induced by scanning tunnelling microscopy. *Journal of microscopy* **2018**.
56. Van Delden, R.A.; Ter Wiel, M.K.; Pollard, M.M.; Vicario, J.; Koumura, N.; Feringa, B.L. Unidirectional molecular motor on a gold surface. *Nature* **2005**, *437*, 1337.
57. Lensen, D.; Elemans, J.A. Artificial molecular rotors and motors on surfaces: STM reveals and triggers. *Soft Matter* **2012**, *8*, 9053–9063.
58. Lu, S.; Huang, M.; Qin, Z.; Yu, Y.; Guo, Q.; Cao, G. Highly ordered molecular rotor matrix on a nanopatterned template: titanyl phthalocyanine molecules on FeO/Pt (111). *Nanotechnology* **2018**, *29*, 315301.
59. Graziano, G. Molecular motors in a tight spot. *Nature Reviews Chemistry* **2018**, *2*, 99.
60. Seldenthuis, J.S.; Prins, F.; Thijssen, J.M.; van der Zant, H.S. An all-electric single-molecule motor. *ACS nano* **2010**, *4*, 6681–6686.
61. Otsuki, J.; Komatsu, Y.; Kobayashi, D.; Asakawa, M.; Miyake, K. Rotational libration of a double-decker porphyrin visualized. *Journal of the American Chemical Society* **2010**, *132*, 6870–6871.
62. Nirmalraj, P.N.; Thompson, D.; Riel, H.E. Capturing the embryonic stages of self-assembly-design rules for molecular computation. *Scientific reports* **2015**, *5*, 10116.
63. Haq, S.; Wit, B.; Sang, H.; Floris, A.; Wang, Y.; Wang, J.; Pérez-García, L.; Kantorovitch, L.; Amabilino, D.B.; Raval, R. A small molecule walks along a surface between porphyrin fences that are assembled in situ. *Angewandte Chemie International Edition* **2015**, *54*, 7101–7105.
64. Nirmalraj, P.; La Rosa, A.; Thompson, D.; Sousa, M.; Martin, N.; Gotsmann, B.; Riel, H. Fingerprinting electronic molecular complexes in liquid. *Scientific reports* **2016**, *6*, 19009.
65. Puigmartí-Luis, J.; Saletra, W.J.; González, A.; Amabilino, D.B.; Pérez-García, L. Bottom-up assembly of a surface-anchored supramolecular rotor enabled using a mixed self-assembled monolayer and pre-complexed components. *Chemical Communications* **2014**, *50*, 82–84.
66. Castelvecchi, D. Drivers gear up for world's first nanocar race. *Nature News* **2017**, *544*, 278.

Preprints (www.preprints.org) | NOT PEER-REVIEWED | Posted: 24 December 2018 doi:10.20944/preprints201812.0290.v1

Peer-reviewed version available at Materials 2019, 12, 382; doi:10.3390/ma12030382

67. Ariga, K.; Mori, T.; Nakanishi, W. Nano Trek Beyond: Driving Nanocars/Molecular Machines at Interfaces. *Chemistry–An Asian Journal* **2018**, *13*, 1266–1278.
68. Rapenne, G.; Joachim, C. The first nanocar race. *Nat. Rev. Mater* **2017**, *2*, 17040.
69. S., T.; Arrhenius, M.; Blanchard-Desce, M.; Dvolaitzky, J.M.; Lehn. Molecular devices: caroviologens as an approach to molecular wires-synthesis and incorporation into vesicle membranes. *Proc. Natl. Acad. Sci. USA* **1986**, *83*, 5355–5359.
70. Li, L.; Lo, W.Y.; Cai, Z.; Zhang, N.; Yu, L. Proton-triggered switch based on a molecular transistor with edge-on gate. *Chemical Science* **2016**, *7*, 3137–3141.
71. Brooke, R.J.; Szumski, D.S.; Vezzoli, A.; Higgins, S.J.; Nichols, R.J.; Schwarzacher, W. Dual Control of Molecular Conductance through pH and Potential in Single-Molecule Devices. *Nano letters* **2018**, *18*, 1317–1322.
72. Nacci, C.; Ample, F.; Bleger, D.; Hecht, S.; Joachim, C.; Grill, L. Conductance of a single flexible molecular wire composed of alternating donor and acceptor units. *Nature communications* **2015**, *6*, 7397.
73. Tricoli, A.; Nasiri, N.; De, S. Wearable and miniaturized sensor technologies for personalized and preventive medicine. *Advanced Functional Materials* **2017**, *27*, 1605271.
74. Yokota, T.; Zalar, P.; Kaltenbrunner, M.; Jinno, H.; Matsuhisa, N.; Kitanosako, H.; Tachibana, Y.; Yukita, W.; Koizumi, M.; Someya, T. Ultraflexible organic photonic skin. *Science advances* **2016**, *2*, e1501856.
75. Lipomi, D.J.; Bao, Z. Stretchable and ultraflexible organic electronics. *MRS Bulletin* **2017**, *42*, 93–97.
76. Rogers, J.A. Wearable electronics: Nanomesh on-skin electronics. *Nature nanotechnology* **2017**, *12*, 839.
77. Thiyagarajan, K.; Jeong, U. Strategies for stretchable polymer semiconductor layers. *Mrs Bulletin* **2017**, *42*, 98–102.
78. Lee, S.; Reuveny, A.; Reeder, J.; Lee, S.; Jin, H.; Liu, Q.; Yokota, T.; Sekitani, T.; Isoyama, T.; Abe, Y.; others. A transparent bending-insensitive pressure sensor. *Nature nanotechnology* **2016**, *11*, 472.
79. Merces, L.; de Oliveira, R.F.; Gomes, H.L.; Bufon, C.C.B. The role of the electrode configuration on the electrical properties of small-molecule semiconductor thin-films. *Organic Electronics* **2017**, *49*, 107–113.
80. Martínez-Domingo, C.; Conti, S.; Terés, L.; Gomes, H.L.; Ramon, E. Novel flexible inkjet-printed Metal-Insulator-Semiconductor organic diode employing silver electrodes. *Organic Electronics* **2018**, *62*, 335–341.
81. Rocha, P.R.; Schlett, P.; Kintzel, U.; Mailänder, V.; Vandamme, L.K.; Zeck, G.; Gomes, H.L.; Biscarini, F.; De Leeuw, D.M. Electrochemical noise and impedance of Au electrode/electrolyte interfaces enabling extracellular detection of glioma cell populations. *Scientific reports* **2016**, *6*, 34843.
82. Pires, F.; Ferreira, Q.; Rodrigues, C.A.; Morgado, J.; Ferreira, F.C. Neural stem cell differentiation by electrical stimulation using a cross-linked PEDOT substrate: expanding the use of biocompatible conjugated conductive polymers for neural tissue engineering. *Biochimica et Biophysica Acta (BBA)-General Subjects* **2015**, *1850*, 1158–1168.
83. Stefani, D.; Perrin, M.; Gutiérrez-Cerón, C.; Aragonès, A.C.; Labra-Muñoz, J.; Carrasco, R.D.; Matsushita, Y.; Futera, Z.; Labuta, J.; Ngo, T.H.; others. Mechanical Tuning of Through-Molecule Conductance in a Conjugated Calix [4] pyrrole. *ChemistrySelect* **2018**, *3*, 6473–6478.
84. Ruiz, M.P.; Aragonès, A.C.; Camarero, N.; Vilhena, J.; Ortega, M.; Zotti, L.A.; Perez, R.; Cuevas, J.C.; Gorostiza, P.; Díez-Pérez, I. Bioengineering a single-protein junction. *Journal of the American Chemical Society* **2017**, *139*, 15337–15346.
85. Cardigos, J.; Ferreira, Q.; Crisóstomo, S.; Moura-Coelho, N.; Cunha, J.P.; Pinto, L.A.; Ferreira, J.T. Nanotechnology-Ocular Devices for Glaucoma Treatment: A Literature Review. *Current eye research* **2018**, pp. 1–7.
86. López-Martínez, M.; Artés, J.M.; Sarasso, V.; Carminati, M.; Díez-Pérez, I.; Sanz, F.; Gorostiza, P. Differential electrochemical conductance imaging at the nanoscale. *Small* **2017**, *13*, 1700958.
87. Sepunaru, L.; Pecht, I.; Sheves, M.; Cahen, D. Solid-state electron transport across azurin: From a temperature-independent to a temperature-activated mechanism. *Journal of the American Chemical Society* **2011**, *133*, 2421–2423.
88. Li, W.; Sepunaru, L.; Amdursky, N.; Cohen, S.R.; Pecht, I.; Sheves, M.; Cahen, D. Temperature and force dependence of nanoscale electron transport via the Cu protein azurin. *ACS nano* **2012**, *6*, 10816–10824.

Preprints (www.preprints.org) | NOT PEER-REVIEWED | Posted: 24 December 2018 doi:10.20944/preprints201812.0290.v1

Peer-reviewed version available at *Materials* **2019**, *12*, 382; doi:10.3390/ma12030382

89. Yu, X.; Lovrincic, R.; Sepunaru, L.; Li, W.; Vilan, A.; Pecht, I.; Sheves, M.; Cahen, D. Insights into solid-state electron transport through proteins from inelastic tunneling spectroscopy: The case of azurin. *ACS nano* **2015**, *9*, 9955–9963.
90. Ouyang, C.; Hashimoto, K.; Tsuji, H.; Nakamura, E.; Majima, Y. Coherent Resonant Electron Tunneling at 9 and 300 K through a 4.5 nm Long, Rigid, Planar Organic Molecular Wire. *ACS Omega* **2018**, *3*, 5125–5130.
91. Steinmann, V.; Moro, L. Encapsulation requirements to enable stable organic ultra-thin and stretchable devices. *Journal of Materials Research* **2018**, *33*, 1925–1936.

Sample Availability: Samples of the compounds ..... are available from the authors.